Publications of the Astronomical Society of the Pacific, 133:014102 (8pp), 2021 January https://doi.org/10.1088/1538-3873/abcd52

New Observations with Gemini and GTC of the VHE Blazar KUV 00311–1938: About Its Redshift and Environment

A. Pichel[1], C. Donzelli[2,3], D. Rosa-Gonzalez[4], M. Fernandez Alonso[1,7], A. C. Rovero[1], H. Muriel[2,3], Y. D. Mayya[4], I. Aretxaga[4], J. Becerra González[5,6], A. Carramiñana[4], J. Mendez-Abreu[5,6], O. Vega[4], E. Terlevich[4], and R. J. Terlevich[4]
[1] Instituto de Astronomía y Física del Espacio (IAFE (CONICET-UBA)), Ciudad Universitaria, CABA, Argentina; anapichel@iafe.uba.ar
[2] Instituto de Investigaciones en Astronomía Teórica y Experimental (CONICET), Córdoba, Argentina
[3] Observatorio Astronómico de Córdoba, Universidad Nacional de Córdoba, Córdoba, Argentina
[4] Instituto Nacional de Astrofísica, Optica y Electrónica, Tonantzintla, 72840 Puebla, Mexico
[5] Instituto de Astrofísica de Canarias, C/Vía Láctea s/n, E-38205 La Laguna, Spain
[6] Departamento de Astrofísica, Universidad de La Laguna, E-38206 La Laguna, Spain
Received 2019 December 20; accepted 2020 November 24; published 2020 December 23

Abstract

Extragalactic very-high-energy (VHE; $E > 100$ GeV) sources are unique objects to study the most powerful particle accelerators in nature, as active galactic nuclei are likely sources of ultra-high-energy cosmic rays. BL Lacertae blazars are the most frequent extragalactic objects found in the VHE gamma-ray catalogs. It is very difficult to estimate their redshifts, considering they have no strong enough optical spectral features, hence ∼20% of them have unknown or poorly constrained redshifts. KUV 00311–1938 is a VHE BL Lacertae blazar, with an uncertain redshift in the range of $0.5 < z < 0.98$. We have obtained deep spectroscopy using Gemini and the GTC telescopes of KUV 00311–1938 and its surroundings with high signal-to-noise ratio in 2016–2017. The lack of features did not allow us to determine the spectroscopic redshift of KUV 00311–1938; nevertheless, we obtain a lower limit of $z \gtrsim 0.475$. We determined the redshifts of 41 galaxies observed in the field-of-view of the blazar and through a population study, identified three pairs and four groups consisting of 3 or 4 members with redshifts in the range $z = 0.1468$–0.4756. Due to the absence of a large group of galaxies, we could not associate KUV 00311–1938 with any of the groups detected.

Key words: BL Lacertae objects: KUV 00311–1938 – Galaxy distances – Galaxy groups

1. Introduction

Blazars are the subclass of active galactic nuclei (AGNs) where the jets are closely aligned with the line of sight (Urry & Padovani 1995). They are powerful and variable sources at all wavelengths, classified on the basis of the presence or absence of emission/absorption lines in their optical spectra: BL Lacertae (BL Lac) objects have very weak or no absorption or emission lines (e.g., Stocke et al. 1991), while flat spectrum radio quasars have strong broad emission lines.

Blazars are the most commonly detected type of extragalactic sources in the gamma-ray sky, with spectra dominated by non-thermal radiation produced by accelerated particles in their jets. At high energies (HE; 20 MeV–300 GeV) the Fourth Fermi-LAT Catalog (Abdollahi et al. 2020) shows 3207 extragalactic sources, 98% of which are blazars. At very high energies (VHE; $E > 100$ GeV) this ratio is 91% for a total of 79 extragalactic sources (the TeV Catalog, Wakely & Horan 2008).

Our current understanding of the EBL is limited, its direct measurement is challenging due to contamination by other backgrounds such as the zodiacal light. However, over the past two decades, multiple and novel methods have been applied to constrain the density of the EBL, and we have now a better insight on the spectral properties of this background (Cooray 2016) and the absorption process of VHE gamma-rays (Dwek & Krennrich 2013). VHE gamma-rays coming from blazars interact via pair production with the EBL photons (e.g., Nikishov 1962; Gould & Schréder 1967), producing imprints in the observed energy spectrum of distant sources. These imprints can be used to estimate the EBL density by using VHE observations of blazars with known redshift (e.g., H. E. S. S. Collaboration & Abdalla 2017; Abeysekara & Archer 2019; Acciari & Ansoldi 2019).

For these studies naturally it is necessary to have not only good observations of VHE blazars but also reliable estimation of their redshifts. Indeed, to understand the particle acceleration mechanisms and the processes of gamma-ray production, it is crucial to know the distance to the source. Unfortunately, most of the VHE blazars are BL Lacs, meaning that there are very weak lines or no features in their optical spectra, so making very difficult the determination of spectroscopic redshift. Moreover, for this kind of blazars the continuum optical/NIR emission of

[7] Now at: Department of Physics, Pennsylvania State University, University Park, PA, USA.

the jet is often much stronger than the one of the host galaxy, preventing also to estimate photometric distances. An alternative is to establish limits to the redshift by analyzing the absorption systems in the line of sight toward the source (Lyα forest, e.g., Furniss et al. 2013) which is not always easy to achieve as it requires UV satellite observations. To estimate the redshift in cases where there was no spectroscopic detection of lines, we have developed a statistical method to determine the confidence level for the blazar to be associated to a system of galaxies with measured redshift. BL Lacs are assumed to be hosted by bright elliptical galaxies, which are confined in groups or clusters of galaxies (e.g., Muriel et al. 2015; Torres-Zafra et al. 2018). The method consists of obtaining spectroscopic observations of the galaxies surrounding the blazar and identifying galaxy groups in the field of view. By performing population studies under the same observing conditions, the probability to associate the blazar with a given group is estimated. This method has been successfully used for PKS 0447–439 (Muriel et al. 2015), PKS 1424+240 (Rovero et al. 2016), and RGB J2243+203 (Rosa González et al. 2019).

KUV 00311–1938 is an unknown redshift BL Lac blazar detected at X-rays by ROSAT (Bauer et al. 2000; Schwope et al. 2000), at HE by Fermi-LAT (Abdo et al. 2009; Ackermann et al. 2011) and VHE by H.E.S.S. (one of the three operational Imaging Atmospheric Cherenkov Telescope—IACT—systems) in 2012 (Becherini et al. 2012). It shows a modest variability in gamma-rays; Fermi-LAT observations during eight years show a variability index of 27.17 (Abdollahi et al. 2020), and observations by H.E.S.S. from December 2009 to December 2014 , show a constant flux within the uncertainties, although the source was detected just above the sensitivity limit at a level of 5.2 standard deviation (Abdalla et al. 2020). Piranomonte et al. (2007) observed the object with the ESO 3.6 m telescope for 900 s in July 2001, estimating a tentative redshift of $z = 0.610$ based on very weak lines present in the optical spectrum (S/N $\sim$ 40 around λ5500). They also estimated a V magnitude of 16.1 from O and E magnitudes in the COSMOS Photometry Catalog. Jones et al. (2009) did not find those weak lines when the object was observed using the 6 dF fiber-fed multi-object spectrograph at the United Kingdom Schmidt Telescope (UKST); they found an unreliable redshift of $z = 0.7635$ (flag $Q = 2$, "unlikely redshift"). Abdalla et al. (2020) have obtained an upper limit of $z < 0.98$ at 95% CL by assuming and intrinsic spectrum derived from fitting a powerlaw to Fermi-LAT observations, modeling the EBL absorption process and comparing the expected absorbed flux with H.E.S.S. observations of KUV 00311-1938.

Pita et al. (2012, 2014) obtained UV to NIR spectroscopy (S/N 80–200 in the visible) using Xshooter on the VLT. The authors found a Mg II doublet corresponding to $z = 0.50507$, later confirmed by Shaw et al. (2013a). The Mg II lines could either correspond to the host galaxy of this object or to an intervening cold system. So, this redshift should be considered as a solid lower-limit of the VHE source. In addition, the absorption lines previously reported by Piranomonte et al. (2007) and Jones et al. (2009) were not confirmed by Pita et al. (2014).

Using the technique described in Sbarufatti et al. (2005), for different host galaxy magnitudes, they estimated a lower limit of the redshift to be 0.5, and from the absence of Lyα absorption lines, an upper limit of $z = 1.54$. All these results suggest KUV 00311–1938 is one of the most distant blazars detected at VHE, in a redshift range poorly populated by other VHE blazars, i.e., $0.506 < z < 0.98$.

As outlined above, blazars detected at VHE gamma-rays are unique objects for the study of several extragalactic astrophysical matters. Unfortunately, present VHE gamma-ray detectors have not enough sensitivity and aperture to populate the VHE catalog with many extragalactic sources; from the 79 detected sources in more than a decade of operation, 73 are blazars (62 BL-Lac, 8 Flat Spectrum Radio Quasar, and 3 of unclear type) and $\sim$20% of them have unknown or poorly constrained redshift. Among the blazars that have an estimated redshift, only 3 are more distant than $z \sim 0.6$ in the VHE catalog and all have been detected under peculiar circumstances, either through lensing with a violent flare (S3 0218+35 at $z = 0.95$, Ahnen et al. 2016) or because the source showed high activity at one or more bands (PKS 1441+25 at $z = 0.94$, Abeysekara et al. 2015; Ahnen et al. 2015; TON 0599 at $z = 0.72$, ATEL#11061, ATEL#11075). Thus, a redshift close to the upper limit reported by Pita et al. (2014) appears unlikely for a blazar detected at VHE.

Therefore, any effort conducting to estimate the redshift of every single object is a welcome contribution.

In this work we present multi-object spectroscopic (MOS) observations of the blazar KUV 00311–1938 and several objects in the field of view from high signal-to-noise ratio data obtained with GMOS-N at Gemini and OSIRIS at GTC. We characterize the surroundings of KUV 00311–1938 and analyze the results from different approaches and techniques related to the redshift of the blazar. In Section 2, we describe the observations and data reduction; in Section 3, we present the analysis and discuss the results, and Section 4 summarizes the results.

2. Observations and Data Reduction

2.1. Gemini

We have obtained medium resolution spectra of KUV 00311–1938 and of 39 objects present in the field that covers $\sim 5 \times 5$ arcmin^2 centered on the blazar. We used the Gemini Multi Object Spectrograph (GMOS) under program GS-2016B-Q-55 (PI: AP). As a first step we obtained a pre-image on 2016 August 4th, consisting of 3×60 s exposures in the Sloan r' (G0326) filter with effective wavelength 630 nm. A binning of 2×2 pixels was used, that results in a spatial scale of 0.16 per pixel. This pre-image was then used to create a multislit mask from a list of selected objects on the image. Figure 1 shows the science targets labeled with their respective slit numbers; slit 1 corresponds to KUV 00311–1938 and slit 39 to the sky. Targets

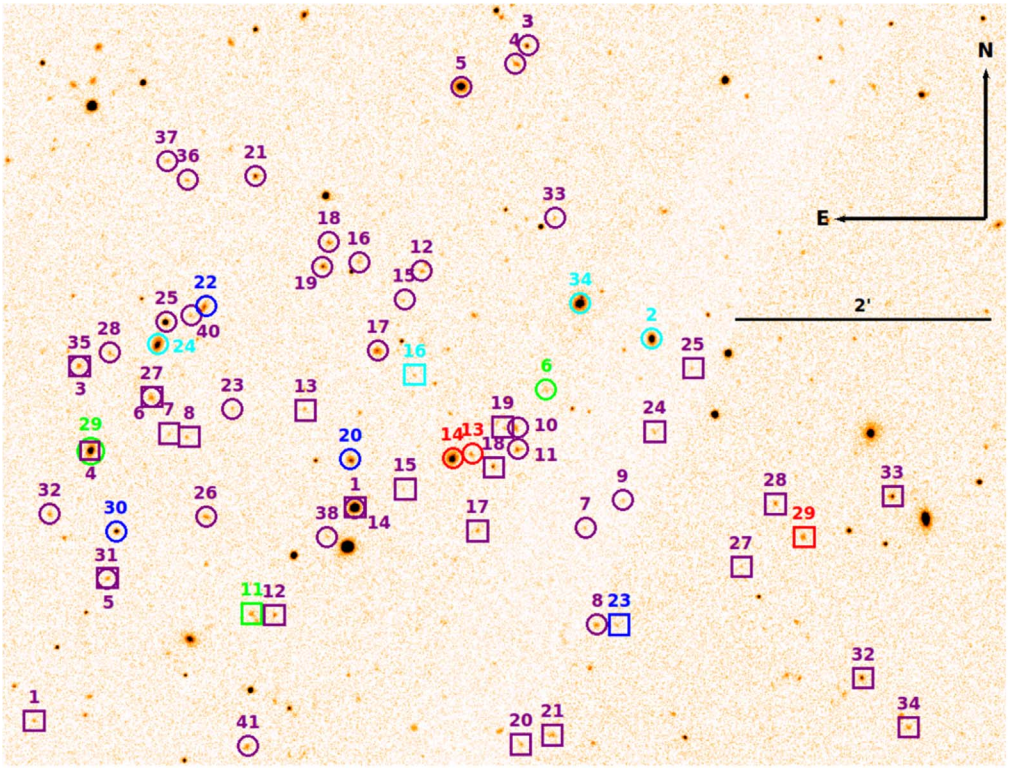

Figure 1. SDSS image showing the field of view for both Gemini and GTC observations. Galaxies selected for spectroscopy are labeled with the slit number: circles for Gemini and squares for GTC. The central position of KUV 00311–1928 corresponds to slit 1 of Gemini and slit 14 of GTC. Groups of galaxies with three or more members (see Table 3) are indicated in cyan for group 1; red for group 2; green for group 3 and blue for group 4. The scale of the image as well as the North and East directions are indicated.

were chosen by eye, considering that their integrated magnitudes were not fainter than $m_r' = 22.5$ in order to obtain spectra with a reasonable S/N ratio. Final placement of slits is controlled by the slit positioning algorithm (SPA) that considers the priority and position of the objects on the image, preserving a minimum separation of two pixels between slits. Slit dimensions were 1″ wide by 4″ long to ensure a good sky subtraction.

Spectra were obtained on 2016 October 5, under excellent seeing conditions (FWHM ∼ 0.″7). A total of 5 × 900 s exposures were obtained at three different central wavelengths (590, 600 and 610 nm) that are used to remove the instrumental gaps between the CCDs. The B600 ± G5323 grating used has a dispersion of ∼0.9 Å per pixel, and a resolution of FWHM ∼ 5 Å. Spectra typically cover the wavelength range 400–700 nm, but the exact range for each spectrum depends on the slit position on the mask. Flat fields, spectra of the spectrophotometric star LTT379, and the copper–argon CuAr lamp were also acquired to perform flux and wavelength calibrations.

Images and spectra were reduced following standard procedures. For this purpose IRAF[8] and Gemini package under IRAF were used. Further details have been discussed in Rovero et al. (2016).

2.2. GTC

Observations of the blazar KUV 00311–1938 and 27 other objects in the field of ∼7.8 × 7.8 arcmin^2 were carried out in service mode with the OSIRIS Multi Object Spectrograph (MOS) installed in the GTC under the program GTC1–17BMEX (PI: DRG). We used the R1000R grism, centered at 7430 Å and covering the range from 5100 to 10000 Å at a dispersion of 2.62 Å per pixel, which gives an effective resolution, measured on strong sky lines, of ∼11 Å. The total observing time was divided in three independent observing blocks (OB) that were observed on 2017 September 13. Each OB consisted of 5 × 545 s exposures on target for removal of cosmic ray hits. The OBs were accompanied by a common set of ancillary files that included observations of the standard star Ross 640, bias, flat-field, and arc lamps. The OBs were observed with air masses between 1.5 and 1.6, under a clear dark night and a seeing of 1.″2. The raw data were reduced using the GTC/MOS pipeline described in Gómez-González et al. (2016). The three different observing blocks were reduced independently, and as a result we obtained three 2D spectral images wavelength and flux calibrated. One of them (OB001) presented a S/N ratio much lower than that of the other

[8] IRAF is distributed by the National Optical Astronomy Observatories, which is operated by the Association of Universities for Research in Astronomy, Inc. (AURA) under cooperative agreement with the National Science Foundation.

two observing blocks (OB002 and OB003) and so it was not used. We averaged the remaining two 2D spectral images to obtain the final one from which we extracted the different spectra using the IRAF task *apall*. Figure 1 shows the GTC science targets labeled with their respective slit numbers; slit 14 corresponds to KUV 00311–1938. Not shown in the figure are slits 2, 9, 10, 22, 26, 30 and 31 which correspond to calibration stars and sky.

3. Results

The GMOS/Gemini observed field objects are listed in Table 1. Target coordinates (J2000.0), Sloan g' and r' magnitudes, and measured redshifts are given. Redshifts were derived using the *fxcor* routine within IRAF. Basically, this task computes radial velocities by deriving the Fourier cross correlation between two spectra. As templates we have used several spectra obtained during previous Gemini runs. However, as *fxcor* does not work properly with noisy spectra, in those cases (at least 3) absorption lines were manually identified to calculate the redshift. Errors in the redshift determination were never higher than 0.0007.

The OSIRIS/GTC objects are listed in Table 2. The same procedure as for the Gemini data was followed to obtain the redshift for all the galaxies in the field of view of KUV 00311–1938. Errors in the redshift determination were small, between 0.0002 and 0.004, and are not included in the table. The redshift of the object at slit 13 was found to be $z = 1.2488$ based on a unique strong wide emission line, which was assumed to correspond to Mg II λ2800. As only one line is present, the redshift is not confirmed.

3.1. Gemini and GTC Optical Spectra

The optical spectra of KUV 00311–1938 obtained with both Gemini and GTC are presented in Figure 2. As we could not determine a good sensitivity function for the Gemini observations, only the normalized spectrum is shown. Fortunately, this does not prevent identification of the lines. The S/N for the spectra was estimated as ∼30, at λ4500 Å, and ∼100, at λ6000 Å.

The spectrum was examined meticulous to detect any emission or absorption lines in the GMOS wavelength range, and we found a featureless spectrum with no visible lines. We have paid particular attention to the Gemini spectrum in the region around ∼4200 Å. We carefully search for the Mg II doublet detected by Pita et al. (2012, 2014) and later confirmed by Shaw et al. (2013a). Pita et al. (2014) report these lines at $\lambda = 4208.7$ Å and $\lambda = 4219.5$ Å which sets $z = 0.50507$. They measured the EWs of these two lines and they obtained 0.164 Å and 0.094 Å, respectively. Unfortunately, the higher value is barely above the detection limit in our spectrum of EW min = 0.10 Å (see Section 3.3) and we can not detect them. The S/N ratio of the Pita et al. (2012, 2014) spectrum in the blue region is at least 3 times higher than ours.

Table 1
Gemini Objects in the Field of KUV 0031-1938 (at Slit 1)

Slit	R.A. (J2000.0)	Decl. (J2000.0)	g'	r'	z
1	00:33:34.38	−19:21:33.1	16.57	16.31	Blazar
2	00:33:23.90	−19:20:08.9	19.36	18.58	0.1458
3	00:33:28.30	−19:17:42.8	22.10	20.51	0.3279
4	00:33:28.66	−19:17:51.9	21.05	20.59	0.1804
5	00:33:30.63	−19:18:03.0	18.99	17.94	0.1233
6	00:33:27.61	−19:20:34.6	22.21	21.69	0.2200
7	00:33:26.26	−19:21:43.3	24.71	22.28	0.6383
8	00:33:25.85	−19:22:31.7	22.19	21.03	⋯
9	00:33:24.91	−19:21:29.4	23.93	22.17	0.5558
10	00:33:28.69	−19:20:53.6	22.30	21.14	0.2919
11	00:33:28.64	−19:21:04.2	21.38	20.25	0.2915
12	00:33:32.00	−19:19:35.2	22.20	21.76	0.4850
13	00:33:30.26	−19:21:06.5	21.98	21.09	0.1608
14	00:33:30.94	−19:21:08.9	18.89	18.49	0.1605
15	00:33:32.66	−19:19:49.8	22.84	21.72	0.3518
16	00:33:34.28	−19:19:31.0	⋯	21.37	⋯
17	00:33:33.59	−19:20:14.8	20.70	19.90	⋯
18	00:33:35.29	−19:19:20.9	22.00	20.76	0.3855
19	00:33:35.49	−19:19:32.8	20.44	20.07	0.1036
20	00:33:34.50	−19:21:09.5	20.25	19.70	0.2376
21	00:33:37.87	−19:18:47.7	21.71	20.20	0.3331
22	00:33:39.68	−19:19:52.9	20.56	19.88	0.2409
23	00:33:38.68	−19:20:43.6	23.13	22.20	⋯
24	00:33:41.33	−19:20:11.9	19.13	18.62	0.1466
25	00:33:41.04	−19:20:00.7	19.02	18.61	star
26	00:33:39.60	−19:21:37.8	21.27	20.35	0.3267
27	00:33:41.54	−19:20:38.3	22.01	20.63	⋯
28	00:33:43.00	−19:20:16.0	21.82	21.05	⋯
29	00:33:43.68	−19:21:04.5	19.38	18.41	0.2168
30	00:33:42.77	−19:21:44.8	21.04	19.85	0.2406
31	00:33:43.08	−19:22:08.4	22.90	21.47	⋯
32	00:33:45.13	−19:21:36.5	21.39	21.22	0.0540
33	00:33:27.33	−19:19:08.9	22.33	21.82	0.2538
34	00:33:26.44	−19:19:51.4	18.61	17.50	0.1474
35	00:33:44.09	−19:20:22.3	21.64	20.97	0.5335
36	00:33:40.28	−19:18:49.8	22.47	21.57	0.4761
37	00:33:40.97	−19:18:40.1	22.31	21.47	0.4752
38	00:33:35.33	−19:21:47.5	22.53	21.80	⋯
40	00:33:40.15	−19:19:57.4	22.85	22.05	⋯
41	00:33:38.17	−19:23:32.4	21.59	20.92	0.5530

Note. Missing slit 39 corresponds to the sky. Column 1: slit number; Cols. 2 and 3: R.A. and decl. (J2000.0); Col. 4 and 5: total g' and r' integrated magnitude; Col. 6: estimated redshift.

The GTC spectrum was carefully inspected seeking for emission and absorption lines without success; we found a completely featureless spectrum. The only lines detected were some telluric lines (Te) and some diffuse interstellar bands (D). The spectrum shows artificial residual features at the wavelength of intense sky emission lines; the effect more severe at wavelengths larger than 8000 Å. Above 8000 Å there is an artificial increment of the flux due to second order effects that are not fully corrected by the observation of the calibration star.

Table 2
OSIRIS/GTC Objects in the Field of KUV 0031-1938 (at Slit 14)

Slit	R.A. (J2000.0)	Decl. (J2000.0)	g'	r'	z
1	00:33:45.7	−19:23:19.8	22.69	21.77	⋯
3	00:33:44.2	−19:20:22.2	21.63	20.97	0.5334
4	00:33:43.6	−19:21:04.4	19.38	18.41	⋯
5	00:33:42.8	−19:22:08.9	22.90	21.47	⋯
6	00:33:41.6	−19:20:38.0	22.01	20.63	⋯
7	00:33:40.9	−19:20:56.5	22.92	21.75	0.5800
8	00:33:40.2	−19:20:58.1	22.42	21.75	0.3856
11	00:33:38.1	−19:22:26.2	22.31	21.24	0.2210
12	00:33:37.2	−19:22:27.0	23.45	21.21	⋯
13	00:33:36.2	−19:20:43.7	22.63	21.84	"1.2488"
14	00:33:34.4	−19:21:33.1	16.57	16.31	Blazar
15	00:33:32.8	−19:21:24.1	24.79	22.55	⋯
16	00:33:32.1	−19:20:27.0	22.51	22.37	0.1469
17	00:33:30.2	−19:21:45.1	22.06	21.24	0.4134
18	00:33:29.6	−19:21:12.8	22.21	20.85	⋯
19	00:33:29.1	−19:20:53.8	23.17	22.30	0.5350
20	00:33:28.5	−19:23:32.6	22.12	21.39	0.4120
21	00:33:27.5	−19:23:27.9	22.58	20.91	⋯
23	00:33:25.0	−19:22:32.4	22.20	21.85	0.2376
24	00:33:23.7	−19:20:55.9	22.61	21.69	0.4554
25	00:33:22.5	−19:20:23.3	22.38	22.35	⋯
27	00:33:20.9	−19:22:03.4	23.51	22.17	⋯
28	00:33:19.6	−19:21:32.0	22.66	21.16	⋯
29	00:33:18.7	−19:21:48.5	21.10	20.73	0.1640
32	00:33:16.5	−19:22:59.4	21.67	20.22	⋯
33	00:33:15.5	−19:21:28.5	21.97	20.05	0.4600
34	00:33:14.9	−19:23:24.4	24.30	20.89	⋯

Note. The missing slits correspond to observation of calibration stars and the sky. Redshift for slit 13 is not confirmed (see text). Column 1: slit number; Cols. 2 and 3: R.A. and decl. (J2000.0); Col. 4 and 5: total g' and r' integrated magnitude; Col. 6: redshift.

Consequently, no spectroscopic redshift could be determined from these observations.

3.2. Search of Clusters in the Field of View of KUV 00311–1938

Typically, BL Lacs are found in elliptical galaxies which in turn are found in groups or clusters of galaxies. Muriel (2016) estimated that at least 2/3 of the BL Lac reside in systems of galaxies. This characteristic has been used to estimate a statistical redshift[9] in cases where the BL Lac shows a featureless spectrum and the parent group/cluster of galaxies is identified. This method has been described and successfully applied previously (Muriel et al. 2015; Rovero et al. 2016; Rosa González et al. 2019).

Figure 3 shows the redshift distribution of the 41 objects in the field of view of KUV 00311–1938 (29 from Gemini, 13 from GTC, with 1 galaxy in common—galaxy at slit 35 of Gemini and 3 of GTC; see Tables 1 and 2). We use the Friend

[9] The mean redshift of the host group/cluster is assigned to the BL-Lac.

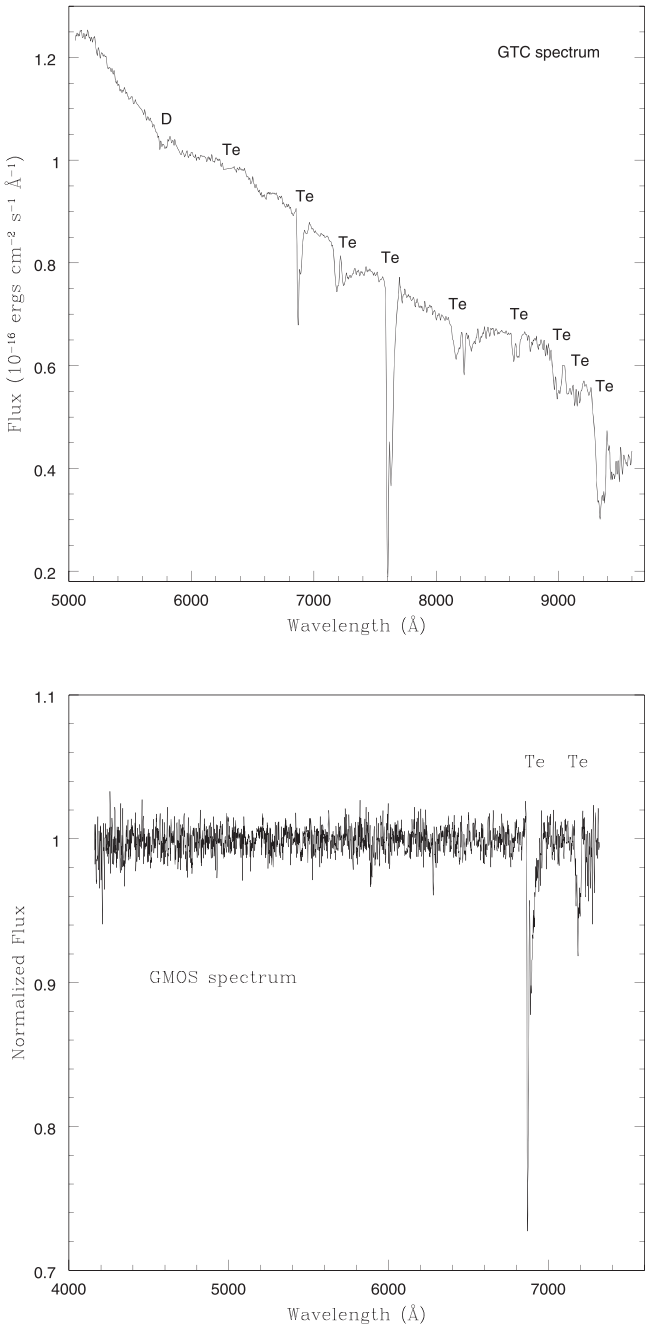

Figure 2. GTC (OSIRIS) spectrum (top) and Gemini (GMOS) normalized spectrum (bottom) of KUV 00311–1938. Telluric (Te) and diffuse interstellar bands (D) are indicated.

of Friend (FOF) algorithm developed by Huchra & Geller (1982) to identify groups (four or more members) and triplets of galaxies. The FOF algorithm groups galaxies into systems using a linking length that depends on the redshift. We use the same procedure as Merchán & Zandivarez (2005), and set the linking length to recover regions with a numerical overdensity of galaxies of 200. Using the FOF algorithm, we found the

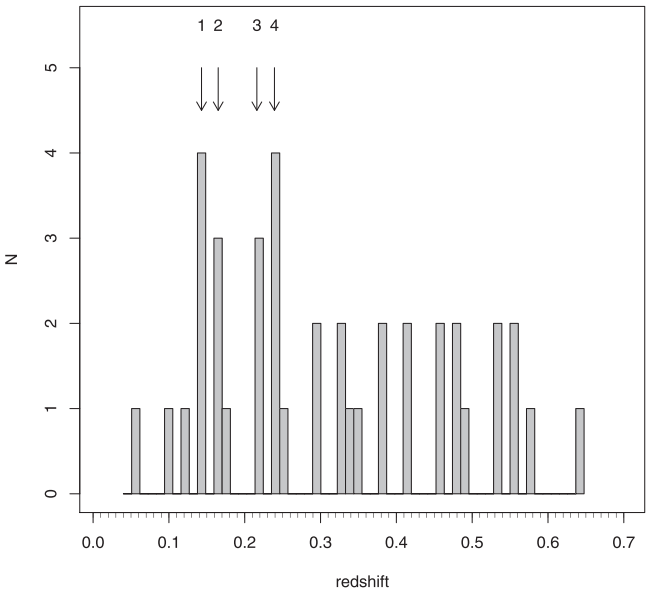

Figure 3. Redshift distribution of galaxies in the field of view of KUV 00311–1938. The arrows indicate the redshift of the groups of 3 and 4 members quoted in Table 3. The galaxy with $z = 1.2488$ was taken out of the histogram to be able to show in more detail the region of z in which all other galaxies were found. Bins containing two galaxies are not necessarily pairs (see text and Table 3).

presence of two triplets and two groups with four members in the redshift range 0.1468–0.2392. Table 3 shows the mean redshift, the virial radius computed as:

$$R_{\rm vir} = \left(\frac{1}{n_{\rm pair}}\Sigma\frac{1}{r_{ij}}\right)^{-1}$$

(where r_{ij} are the mutual projected angular distances between all the possible pairs of galaxies in the group, see Nurmi et al. 2013) and the line of sight velocity dispersion computed using the Gapper estimator by Beers et al. (1990). The velocity dispersion is given by:

$$\sigma = \frac{\sqrt{\pi}}{(1+z)n(n-1)}\sum_{i=1}^{n-1} w_i g_i$$

where $w_i = i(n-i)$ are the weights and $g_i = v_{i+1} - v_i$, and v_i are the ordered radial velocities. The Gapper Estimator is insensitive to outliers and thus accurately reproduces the true velocity dispersion of the system.

We also search for pairs (close pairs) of galaxies following the criteria used by Alpaslan et al. (2015) (see also Coenda et al. 2019). According to these authors, two galaxies with velocity separation $\leqslant 1000 \times (1+z)$ km s^{-1} and projected separation $\leqslant 1$ Mpc (0.1 Mpc), are considered to be pairs (close pairs). Using these criteria, we found two close pairs at $z = 0.2917$ and 0.4756, respectively, and a pair of galaxies at $z = 0.4127$. The lack of a rich group or cluster of galaxies in the field of view of KUV 00311–1938 together with the large number of small groups/triplets makes it impossible to associate the blazar with any of those systems at a reasonable confidence level.

Table 3
Groups of Galaxies with 2, 3 and 4-members in the Field of View of KUV 00311–1938

Group Number	$\langle z \rangle$	σ_r (km s^{-1})	$r_{\rm vir}$/Pair Separation (Mpc)	Number of Members	Slits (Gemini/GTC)
1	0.1468	132	0.25	4	2, 24, 34/16
2	0.1618	501	0.07	3	13, 14/29
3	0.2193	540	0.58	3	6, 29/11
4	0.2392	441	0.57	4	20, 22, 30/23
5	0.2917	⋯	0.045	2	10, 11/
6	0.4127	⋯	0.608	2	/17, 20
7	0.4756	⋯	0.083	2	36, 37/

Note. Column 1: group number; Col. 2: mean redshift; Col. 3: line of sight velocity dispersion; Col. 4: virial radius; Col. 5: number of members for each group; Col. 6: Gemini or GTC slit number.

3.3. Constraints on the Redshift of KUV 00311–1938

Non-thermal radiation from the jet of the blazar is often featureless and usually brighter than the luminosity of the host galaxy, preventing the detection of spectral features. When this happens, and assuming that all BL Lacs are hosted by a bright elliptical galaxy (BEG) (Falomo et al. 1997; Jannuzi et al. 1997), it is possible to set a lower limit to the blazar distance by assigning a luminosity to the host galaxy. To do that, we first selected the spectrum of the most luminous and closest galaxy of the observed field; this is the elliptical galaxy on slit 2 of Gemini (see Table 1) with $z = 0.1458$ and $M = -20.63$ in the r'-band. The spectrum of this galaxy shows several prominent lines, Ca II K&H at 3934 and 3969 Å, respectively, Hβ at 4861 Å and Na I D at 5890 Å. For the BEG host we assume an absolute magnitude $M = -22.5$ (Shaw et al. 2013b) and the spectrum of the selected galaxy was scaled accordingly. This spectrum is added to that of KUV 00311–1938 to check if the absorption lines are still observable. The idea is to dim the host galaxy spectrum by a distance factor and repeat this process until the absorption lines are no longer detectable. In principle, this is a reliable lower limit for the blazar distance. To properly identify absorption lines we followed the method described by Sbarufatti et al. (2006): we have computed the minimum measurable equivalent width (EW) in our spectra to be $\mathrm{EW_{min}} = 0.10$ Å. $\mathrm{EW_{min}}$ is defined as two times the rms of the distribution of all EW values measured dividing the normalized spectrum into 5 Å wide bins which is the spectral resolution of the used GMOS configuration. It is clear that the

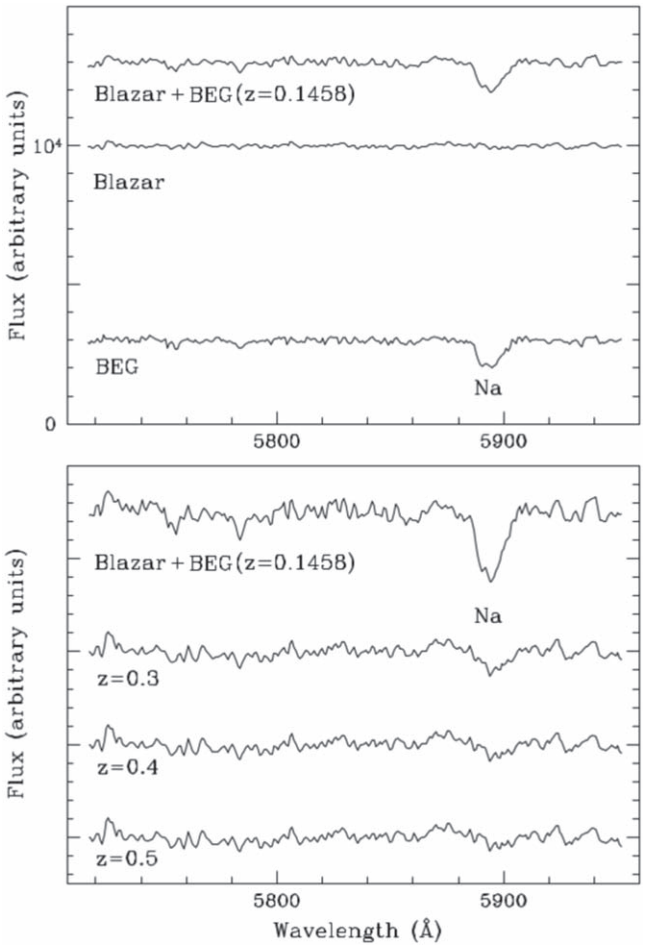

Figure 4. Top panel: spectra for the blazar and the assumed host, a bright elliptical galaxy (BEG), at $z = 0.1458$. The Na I D line at 5890 Å is visible. The sum of both spectra is also shown. Lower panel: the result of adding the host galaxy spectrum at $z = 0.3$, 0.4 and 0.47, to the blazar spectrum. All spectra are shown in their rest frame, shifted in flux for clarity.

total amplitude error for the measured EW is our detection limit at two times the rms, that corresponds to 0.10 Å, and then the associated error to the EW measurements is ±0.05 Å.

Results of this method can be appreciated in Figure 4 where the wavelength range at the more prominent absorption line, Na I D, is plotted. The top figure shows the normalized spectra of KUV 00311–1938 (Gemini) and the chosen host galaxy (BEG) at $z = 0.1458$. The sum of both spectra (the testing spectrum) is also shown. The bottom figure shows the test spectrum built with the BEG spectrum for redshifts in the range $z = 0.1458$–0.5. The EW for the Na line in those spectra are: 0.36 Å for $z = 0.3$; 0.17 Å for $z = 0.4$, and 0.09 Å for $z = 0.5$. We have also computed the EW for the Na line at $z = 0.45$ and 0.475, and we find EW = 0.12 Å and 0.10 Å, respectively. We can then conclude that the Na I line is no longer observed for $z > 0.475$ using this analysis, and therefore we adopt this redshift as a lower limit for the distance to KUV 00311–1938. Even if the method is approximate, it has been proven to work, and the obtained result is in good agreement with that of Pita et al. (2014) who detected the Mg II doublet (λ 2795, 2803 Å) at $z = 0.50507$.

4. Discussion and Remarks

We present here new spectroscopic data on the BL Lac blazar KUV 00311–1938 and of several other galaxies present in the field of view of the observations, obtained with Gemini-GMOS in 2016 over the spectral range 4000–7000 Å, and with the GTC-OSIRIS spectrograph in 2017 covering the 5100–10000 Å range.

Our optical spectra confirm previous results about the lack of emission or absorption lines in the spectrum of KUV 00311–1938. Given the absence of lines we have performed a simulation to estimate a lower limit for the redshift. Using the Sbarufatti technique assuming the blazar is hosted by a massive elliptical galaxy of $M = -22.5$, typical for these sources, a simulated spectrum was created by adding the observed blazar spectrum to that of the (much dimmer) elliptical galaxy placed at the redshift under study. By analyzing how its spectral lines would diminish with distance, we were able to estimate a lower limit $z > 0.475$ for the blazar which is in accordance with a previous result obtained by Pita et al. (2014).

From our Gemini observations we could not detect the Mg II doublet line in the spectrum reported by Pita et al. (2014) using data from Xshooter VLT. We can attribute this to the low signal to noise of the Gemini data around $\lambda \sim 4200$ Å, 3 times dimmer than Pita et al. (2014).

If BL Lac objects are hosted by massive elliptical galaxies, as they are usually found in groups or clusters of galaxies, it is natural to assume that KUV 00311–1938 is a member of a group. We studied the environment of the object from 41 galaxies observed in the field of view of the blazar. We measured their spectroscopic redshifts and found 3 pairs of galaxies and 4 different groups with 3 or 4 members each, located at redshifts between 0.1468 and 0.4756. Our technique to associate KUV 00311–1938 to one specific group was not possible to perform with a reasonable confidence level; the presence of several minor groups found in the surroundings of KUV 00311–1938 prevented us to get a good probability value for the association. In an effort to correlate the results of the galaxy associations with the lower limit of $z > 0.5$ found by Pita et al. (2014), we could not find any group of galaxies, only individual galaxies were detected. This could be the result of the fact that the telescopes we used limit the luminosity of objects to those not much farther than $z \sim 0.6$, and/or that BL Lac objects have a $\lesssim 1/3$ probability of not being associated with a group of galaxies (Muriel 2016).

To summarize, we have determined the redshifts of 41 galaxies observed in the field of view of KUV 00311–1938. We confirm that the lower limit for the blazar is $z > 0.475$.

We sincerely thank an anonymous referee for invaluable comments and suggestions. This work is based on observations obtained at the Gemini Observatory, which is operated by the Association of Universities for Research in Astronomy, Inc., under a cooperative agreement with the NSF on behalf of the Gemini partnership: the National Science Foundation (United States), the National Research Council (Canada), CONICYT (Chile), the Australian Research Council (Australia), Ministério da Ciência, Tecnologia e Inovação (Brazil) and Ministerio de Ciencia, Tecnología e Innovación Productiva (Argentina). Based on observations made with the Gran Telescopio Canarias (GTC), instaled in the Spanish Observatorio del Roque de los Muchachos of the Instituto de Astrofísica de Canarias, in the island of La Palma. This work has been partially supported by grants from Consejo Nacional de Investigaciones Científicas y Técnicas de la República Argentina (CONICET) and Secretaría de Ciencia y Tecnología de la Universidad de Córdoba. A.P., A.C.R., H.M. and C.D. are members of "Carrera del Investigador Científico" of CONICET, Argentina. D.R.G. is partly supported by CONACyT (Mexico) through research grant CB-A1-S-22784.

ORCID iDs

J. Mendez-Abreu https://orcid.org/0000-0002-8766-2597
O. Vega https://orcid.org/0000-0002-2852-9737

References

Abdalla, H., Adam, R., Aharonian, F., et al. 2020, MNRAS, 494, 5590
Abdo, A. A., Ackermann, M., Ajello, M., et al. 2009, ApJ, 700, 597
Abdollahi, S., Acero, F., Ackermann, M., et al. 2020, ApJS, 247, 33
Abeysekara, A. U., Archambault, S., Archer, A., et al. 2015, ApJL, 815, L22
Abeysekara, A. U., & Archer, A. 2019, ApJ, 885, 150
Acciari, V. A., & Ansoldi, S. 2019, MNRAS, 486, 4233
Ackermann, M., Ajello, M., Allafort, A., et al. 2011, ApJ, 743, 171
Ahnen, M. L., Ansoldi, S., Antonelli, L. A., et al. 2015, ApJL, 815, L23
Ahnen, M. L., Ansoldi, S., Antonelli, L. A., et al. 2016, A&A, 595, A98
Alpaslan, M., Driver, S., Robotham, A. S. G., et al. 2015, MNRAS, 451, 3249
Bauer, F. E., Condon, J. J., Thuan, T. X., & Broderick, J. J. 2000, ApJS, 129, 547
Becherini, Y., Boisson, C., Cerruti, M. & H. E. S. S. Collaboration 2012, in AIP Conf. Ser. 1505, Discovery of VHE γ-ray emission from the very distant BL Lac KUV 00311-1938 by H.E.S.S, ed. F. A. Aharonian, W. Hofmann, & F. M. Rieger (Melville, NY: AIP), 490
Beers, T. C., Flynn, K., & Gebhardt, K. 1990, AJ, 100, 32
Coenda, V., Mast, D., Martínez, H. J., Muriel, H., & Merchán, M. E. 2019, A&A, 621, A98
Cooray, A. 2016, RSOS, 3, 150555
Dwek, E., & Krennrich, F. 2013, APh, 43, 112
Falomo, R., Urry, C. M., Pesce, J. E., et al. 1997, ApJ, 476, 113
Furniss, A., Williams, D. A., Danforth, C., et al. 2013, ApJL, 768, L31
Gómez-González, V. M. A., Mayya, Y. D., & Rosa-González, D. 2016, MNRAS, 460, 1555
Gould, R. J., & Schréder, G. P. 1967, PhRv, 155, 1404
H. E. S. S. Collaboration, Abdalla, H. 2017, A&A, 606, A59
Huchra, J. P., & Geller, M. J. 1982, ApJ, 257, 423
Jannuzi, B. T., Yanny, B., & Impey, C. 1997, ApJ, 491, 146
Jones, D. H., Read, M. A., Saunders, W., et al. 2009, MNRAS, 399, 683
Merchán, M. E., & Zandivarez, A. 2005, ApJ, 630, 759
Muriel, H. 2016, A&A, 591, L4
Muriel, H., Donzelli, C., Rovero, A. C., & Pichel, A. 2015, A&A, 574, A101
Nikishov, A. I. 1962, J. Exp. Theor. Phys., 14, 393
Nurmi, P., Heinämäki, P., Sepp, T., et al. 2013, MNRAS, 436, 380
Piranomonte, S., Perri, M., Giommi, P., Landt, H., & Padovani, P. 2007, A&A, 470, 787
Pita, S., Goldoni, P., Boisson, C., et al. 2012, in AIP Conf. Ser. 1505, High energy blazars spectroscopy with X-shooter on the VLT, ed. F. A. Aharonian, W. Hofmann, & F. M. Rieger (Melville, NY: AIP), 566
Pita, S., Goldoni, P., Boisson, C., et al. 2014, A&A, 565, A12
Rosa González, D., Muriel, H., Mayya, Y. D., et al. 2019, MNRAS, 482, 5422
Rovero, A. C., Muriel, H., Donzelli, C., & Pichel, A. 2016, A&A, 589, A92
Sbarufatti, B., Falomo, R., Treves, A., & Kotilainen, J. 2006, A&A, 457, 35
Sbarufatti, B., Treves, A., & Falomo, R. 2005, ApJ, 635, 173
Schwope, A., Hasinger, G., Lehmann, I., et al. 2000, AN, 321, 1
Shaw, M. S., Filippenko, A. V., Romani, R. W., Cenko, S. B., & Li, W. 2013a, AJ, 146, 127
Shaw, M. S., Romani, R. W., Cotter, G., et al. 2013b, ApJ, 764, 135
Stocke, J. T., Morris, S. L., Gioia, I. M., et al. 1991, ApJS, 76, 813
Torres-Zafra, J., Cellone, S. A., Buzzoni, A., Andruchow, I., & Portilla, J. G. 2018, MNRAS, 474, 3162
Urry, C. M., & Padovani, P. 1995, PASP, 107, 803
Wakely, S. P., & Horan, D. 2008, Proc. ICRC, 3, 1341